

## Electron Density Measurements in the TRIAM-1 Tokamak

Mitarai, Osamu

JSPS : Post Doctoral Fellowships | Research Institute for Applied Mechanics, Kyushu University

Nakashima, Hisatoshi

Research Institute for Applied Mechanics, Kyushu University : Technical Assistant

Nakamura, Kazuo

Research Institute for Applied Mechanics, Kyushu University : Research Associate

Hiraki, Naoji

Research Institute for Applied Mechanics, Kyushu University : Research Associate

他

<https://doi.org/10.15017/1544155>

---

出版情報 : Reports of Research Institute for Applied Mechanics. 27, pp.147-158, 1980-02. 九州大学応用力学研究所

バージョン :

権利関係 :

④

With Compliments

**Electron Density Measurements in the  
TRIAM-1 Tokamak**

By

Osamu MITARAI, Hisatoshi NAKASHIMA,  
Kazuo NAKAMURA, Naoji HIRAKI  
Kazuo TOI, Yoshinobu KAWAI  
and Satoshi ITOH



Reprinted from Reports of Research Institute  
for Applied Mechanics, Kyushu University  
Vol. XXVII, No. 86, February 1980

## ELECTRON DENSITY MEASUREMENTS IN THE TRIAM-1 TOKAMAK

Osamu MITARAI\*, Hisatoshi NAKASHIMA\*\*,  
KAZUO NAKAMURA\*\*\*, Naoji HIRAKI\*\*\*\*,  
Kazuo TOI\*\*\*\*, Yoshinobu KAWAI\*\*\*\*  
and Satoshi ITOH\*\*\*\*\*

Electron density measurements in the TRIAM-1 tokamak are carried out by a 140 GHz microwave interferometer. To follow rapid density variations, a high-speed direct-reading type interferometer is constructed. The density of  $(1-20) \times 10^{13} \text{cm}^{-3}$  is measured.

**Key words:** Density, interferometer, microwave, tokamak

### 1. Introduction

A zebra-stripe interferometer<sup>1)</sup> has widely been used to measure an electron density in a tokamak plasma. In the case of high density, however, it may be difficult to measure the density by the Zebra-stripe interferometer because of the numerous number of fringes. To overcome such a difficulty, three kinds of the direct-reading type interferometers; two-level modulation method<sup>2)</sup>, tri-level modulation method<sup>3)</sup> and method without modulation<sup>4)</sup>, have been proposed so far. The two-level modulation method has a very simple modulation wave form (square wave) in comparison with the tri-level modulation method and does not require to reconstruct a reference path, so that we adopted the two-level modulation method to measure the TRIAM-1 tokamak<sup>5)</sup> which has a large  $B_t/R$  value, providing a high density plasma<sup>6)</sup>.

\* JSPS Post Doctoral Fellowships (General), Research Institute for Applied Mechanics, Kyushu University.

\*\* Technical Assistant, Research Institute for Applied Mechanics, Kyushu University.

\*\*\* Research Associate, Research Institute for Applied Mechanics, Kyushu University.

\*\*\*\* Associate Professor, Research Institute for Applied Mechanics, Kyushu University.

\*\*\*\*\* Professor, Research Institute for Applied Mechanics, Kyushu University.

Since rapid current rise discharges have been carried out in the TRIAM-1 tokamak, the density rise rate at the initial phase of the discharge is very fast as compared with that of medium size tokamaks. Therefore we constructed a high-speed direct-reading type interferometer to measure the density in the TRIAM-1 tokamak plasma. In this paper we describe about this interferometer and present the results of the measurements.

In section 2, we review a principle of the density measurement. The experimental apparatus are described in section 3. In section 4, the experimental results are presented and discussed.

## 2. Basic Considerations

### 2.1 Electron density measurement

The dispersion relation of an ordinary mode propagating through a collisional plasma is given as follows<sup>1)</sup>:

$$n^2 = \frac{1}{2} \left[ 1 - \frac{(\omega_p/\omega)^2}{1 + (\nu/\omega)^2} + \left\{ \left[ 1 - \frac{(\omega_p/\omega)^2}{1 + (\nu/\omega)^2} \right]^2 + \left[ \frac{(\omega_p/\omega)^2}{1 + (\nu/\omega)^2} \right]^2 \left( \frac{\nu}{\omega} \right)^2 \right\}^{1/2} \right] \quad (1)$$

where  $n$ ,  $\omega_p$ ,  $\omega$  and  $\nu$  are refractive index, electron plasma frequency, incident wave frequency and collision frequency, respectively. For a collisionless plasma, we have the following well-known relation:

$$n^2 = 1 - (\omega_p/\omega)^2 = (K_p/K_0)^2 \quad (2)$$

where  $K_p$  and  $K_0$  are the wave number of the ordinary mode, respectively.

On the other hand, the number of fringe  $m$  is defined as

$$\begin{aligned} m &= \Delta\phi/2\pi = \int_{-a}^a (K_0 - K_p) dx \\ &= \int_{-a}^a [1 - \sqrt{1 - n(x)/n_c}] \frac{dx}{\lambda} \end{aligned} \quad (3)$$

where  $n(x)$ ,  $n_c$ ,  $\lambda$  and  $a$  are an electron density at  $x$ , cut-off density, incident wavelength and plasma radius, respectively. Equation (3) demonstrates that the number of the fringe  $m$  depends on the profile of the electron density. Here, we write down the relationship between  $m$  and a line density  $\bar{n}$  for three types of density distributions:

(i)  $n(x) = (3/2)\bar{n}(1 - x^2/a^2)$  [parabolic]

$$\begin{aligned} m &= 3a/\lambda - a/(2\lambda)(c^{-1} - c) [\log(1+c) - \log(1-c)] \\ c &= (3\bar{n}/2n_c)^{1/2} \end{aligned} \quad (4)$$

(ii)  $n(x) = \bar{n}$  [flat]

$$m = (2a/\lambda) [1 - (1 - \bar{n}/n_c)^{1/2}] \quad (5)$$

(iii)  $n(x) = 3\bar{n}x^2 a^{-2}$  [hollow]

$$m = 2a/\lambda - (a/\lambda) [(1 - 3\bar{n}/n_c)^{1/2} + (3\bar{n}/n_c)^{-1/2} \sin^{-1}(3\bar{n}/n_c)^{1/2}] \quad (6)$$

In Fig. 1 are plotted these results in the case of the microwave frequency of 140 GHz. It is found from this figure that the average line density depends on the profile and the maximum number of fringe increases as the density profile becomes broad. To investigate these relations, we assume  $n(x) = n_c(1 - (x/a)^\beta)$  and obtained the following relation :

$$m_{\max} = \frac{2a}{\lambda} \frac{\beta}{\beta + 2} \quad (7)$$

where  $m_{\max}$  is the maximum number of the fringe. This is plotted in Fig. 2.

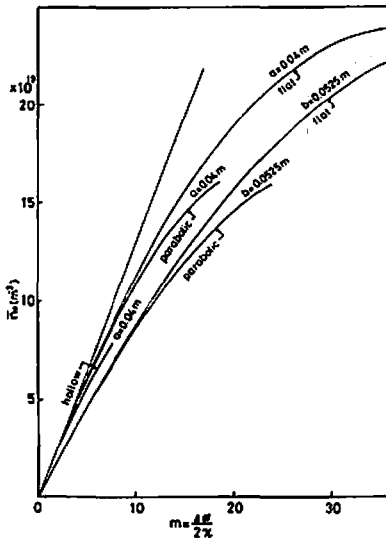


Fig. 1 The average line density v. s. the number of fringe.

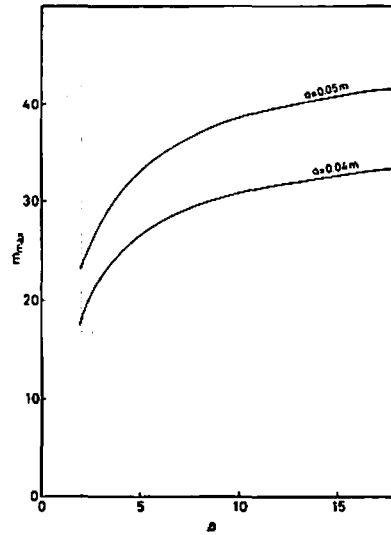


Fig. 2 The maximum number of fringe v. s. the profile coefficient  $\beta$ .

### 2. 2 Microwave refraction

A wave refraction angle for a cylindrical plasma was derived by J. Shmoys<sup>2)</sup>. For the case  $n = n_0(1 - r^2/a^2)$ , the following relation is obtained:

$$\theta_{ref}(b) = \sin^{-1} \frac{n_0}{n_c} \left[ \frac{(b/a)^2 - (b/a)^4}{(n_0/n_c)(b/a)^2 + (1 - n_0/n_c)^2/4} \right]^{1/2} \quad (8)$$

where  $\theta_{ref}$ ,  $n_0$ , and  $b$  are a refraction angle, peak density and impact parameter, respectively. Using  $n_0/n_c = (\omega_p/\omega)^2$ , we calculated  $\theta_{ref}(b)$ . In Fig. 3 is shown the wave refraction angle for the microwave frequency of 140 GHz. When the impact parameter is equal to 0, the refraction angle becomes zero. If the plasma position is displaced, the output signal will decrease for this effect.

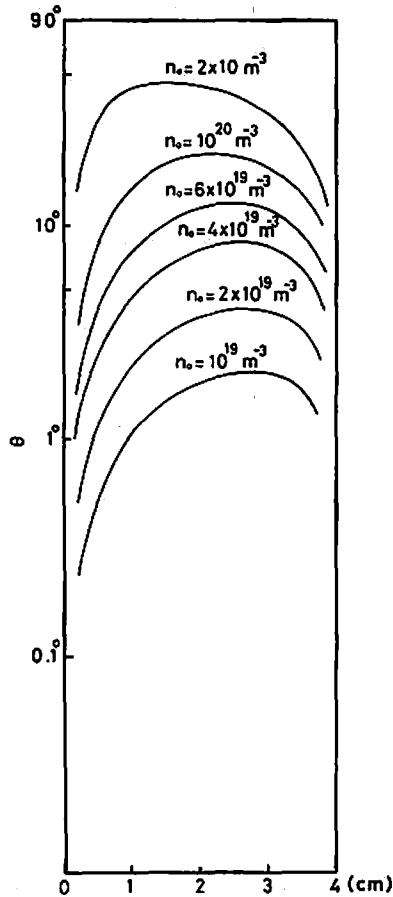


Fig. 3 The microwave refraction angle for a 140 GHz microwave.

### 3. Experimental Apparatus

#### 3.1 A microwave circuit

Figure 4 shows a microwave circuit diagram used here. A 139 GHz microwave emitted from the klystron (VRT-2121 A, Varian) is divided into a plasma path and reference one. The plasma path consists of the

X-band straight waveguides, taper waveguides, H-plane bends, circular horns and E-H tuner. The reference path consists of the attenuator, phase shifter, T band waveguides and directional coupler. The signals of the plasma path and reference one are mixed by the directional coupler and divided into the two diode detectors. The outputs of the detectors are conducted into the direct-reading type interferometer. The alignment of the horns and waveguides should be carefully performed using the levels.

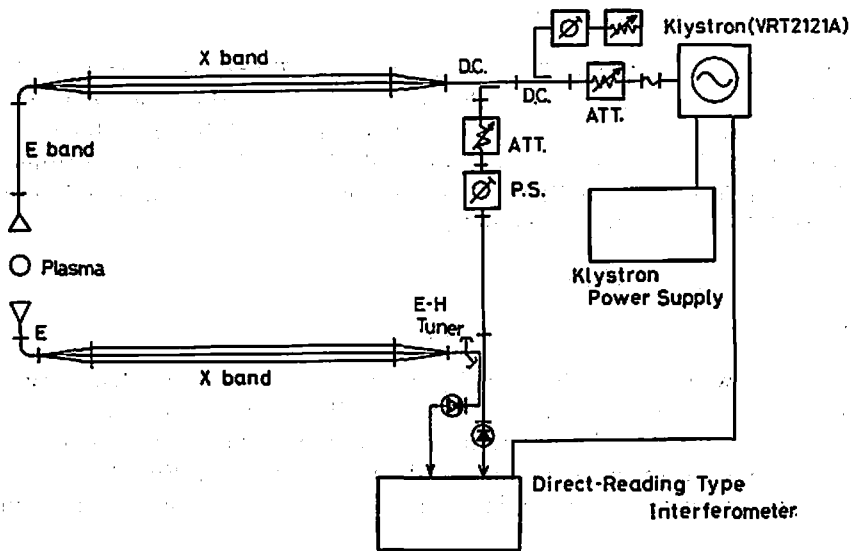


Fig. 4 The microwave circuit measuring the electron density in the TRIAM-1 tokamak.

### 3.2 Direct-reading type interferometer

#### 3.2.1 Principle of the direct-reading type interferometer

Principle of the direct-reading type interferometer was described in detail in the reference 2). Here we review it. We apply the square wave modulation to the klystron:

$$V(t) = V_m \quad \text{at } 0 \leq t < T,$$

and

$$V(t) = 0 \quad \text{at } T \leq t < 2T,$$

where  $1/2T$  is the modulation frequency.

In the case of VRT-2121 A, a reflector modulation sensitivity is 3 MHz/V. The phase difference between the plasma path and the reference one is given by<sup>6)</sup>

$$\Delta\phi = 2\pi \frac{l_p - l_r}{\lambda_g} \left( \frac{\lambda_g}{\lambda} \right)^2 \frac{\Delta f}{f}, \tag{9}$$

where  $l_p$ ,  $l_r$ ,  $\lambda_g$ ,  $\lambda$  and  $\Delta f$  the plasma path length, reference path length, wavelength in the waveguide, wavelength in the free space and modulation frequency, respectively and  $f = \omega/2\pi$ . Here  $\Delta\phi$  is adjusted to  $\pi/2$  by changing the applied modulation voltage. For the present case where  $l_p - l_r = 5$  m,  $f = 139$  GHz,  $\Delta f = 3 \times 10^6 V_m$ ,  $\lambda = 2.158$  mm,  $\lambda_g = 2.160$  mm (for the X band), we obtain  $\Delta\phi = \pi/2$ , when  $V_m = 5$  V are chosen.

If the density increases linearly, the output signal of the detector is expressed by

$$V_D = \sin(\psi_p(t) + \Delta\phi) \quad (11)$$

where  $\Delta\phi = \pi/2$  for  $0 \leq t < T$ ,  $\Delta\phi = 0$  for  $T \leq t < 2T$  and  $\psi_p(t)$  is the phase change due to plasma. Since the output signal of the diode detector is small, we must amplify it. The output of the amplifier as shown in is divided into the summing amplifier and the analog switch connected with the differential amplifier. The output of the summing amplifier and differential one can be expressed as

$$V_{\text{sum}} = \sqrt{2} \sin(\psi_p(t) + \pi/4) \quad (12)$$

and  $V_{\text{diff}} = \sqrt{2} \sin(\psi_p(t) - \pi/4)$ . (13)

We can know whether the density increases or not by observing the phase relation between  $V_{\text{sum}}$  and  $V_{\text{diff}}$ . The comparator-analog switch system discriminates the above phase relation. We show the example of this relation in Figs. 6 and 7. It is found from Fig. 6 that it is necessary to make careful adjustment of the zero crossing not to miscount.

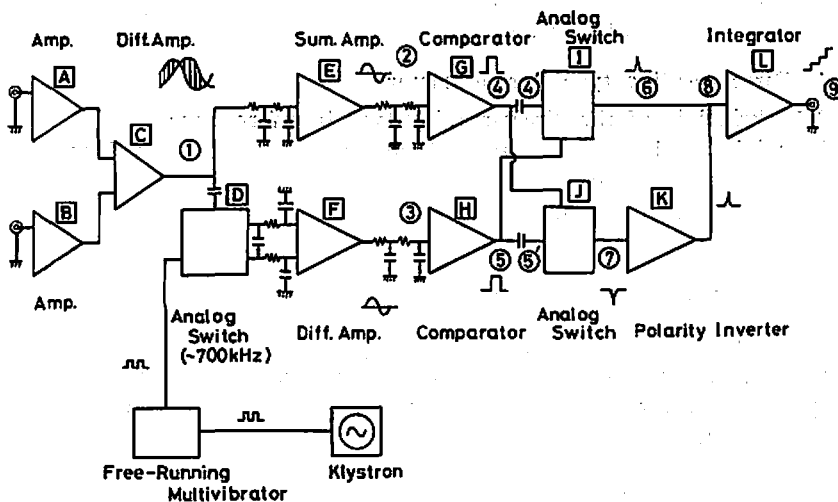


Fig. 5 The block diagram of the direct-reading type interferometer.



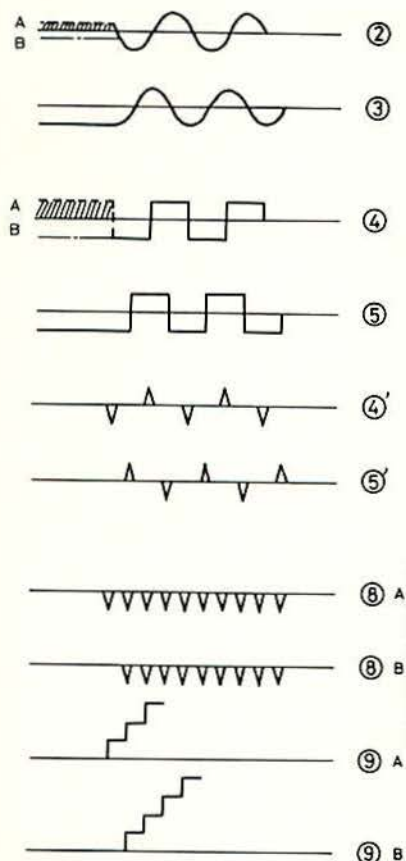


Fig. 6 The relation of the summing amplifier (2) and differential amplifier (3) output signal to the integrator output signal (9) in the case of the linearly increasing density.

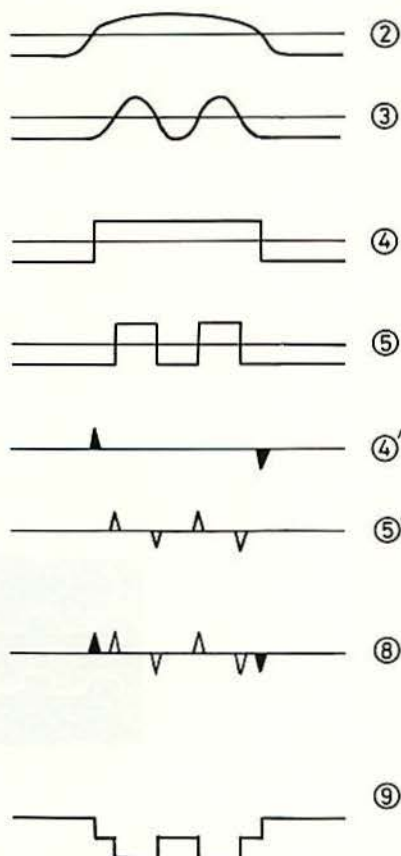


Fig. 7 The relation of the summing amplifier (2) and differential amplifier (3) output signal to the integrator output signal (9) in the case of a fluctuating density.

### 3.2.2 Construction and operation of the high-speed direct-reading type interferometer

To measure the rapid density variation by this interferometer, we constructed the circuit which had a higher modulation frequency, higher speed amplifier and the RC filter with a higher cut-off frequency. Since the frequency characteristic of this system was limited by that of the diode detector, we tested this using a signal generator. The results are shown in Figs. 8 and 9 (1). It is found from this figure that the maximum modulation frequency is about 700 kHz, as far as this diode detector is used. Thus, we selected the modulation frequency of 700kHz.

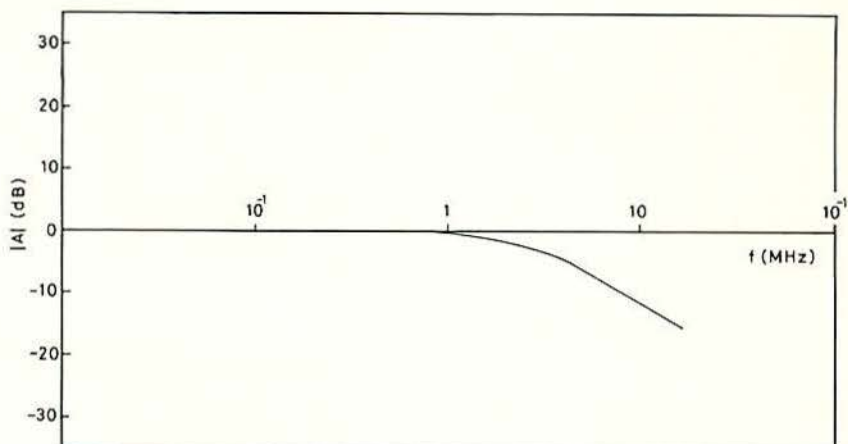
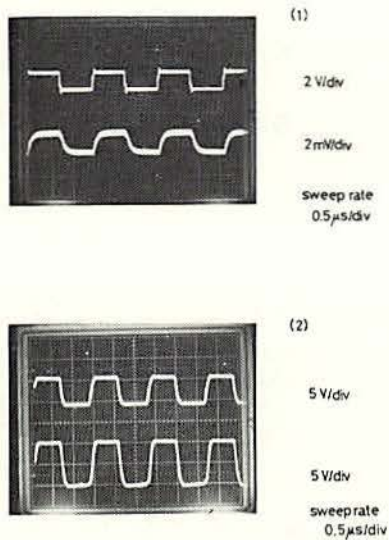
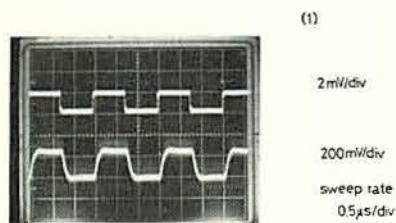


Fig. 8 The frequency characteristic of the diode detector.



- Fig. 9 (1) The upper trace is the modulation voltage applied to the klystron and the lower trace the output of the diode detector.
- (2) The upper trace is the input voltage into an analog switch and the lower trace the modulation voltage applied to the klystron.

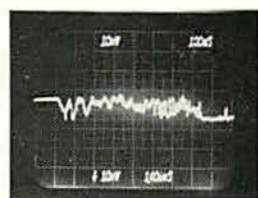
The square wave which is shown in Fig. 9 (2) was generated by the high-speed free-running multivibrator ( $\mu A$  773DC). We used the high-speed operational amplifier (Teledyne, 1321). The frequency response



(1)

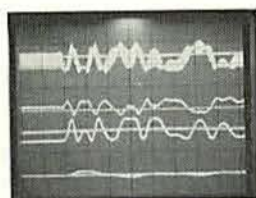
2mV/div

200mV/div

sweep rate  
0.5μs/div

(1) Shot No. 11267

10mV/div

sweep rate  
100μs/div

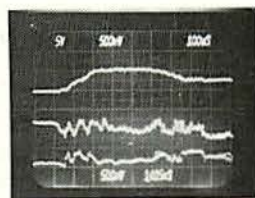
(2)

(A) 0.1V/div

(B) 2V/div

(C) 2V/div

(D) 2V/div

sweep rate  
20ms/div

(2) Shot No. 11287

(A) 0.5V/div

(B) 5V/div

(C) 5V/div

sweep rate  
100μs/div

Fig. 10(1) The frequency response of the amplifier.

- (2) A test of the direct-reading type interferometer by a method vibrating one horn. (A) An output signal of the differential amplifier [C]. (B) An output of the summing amplifier. (C) An output of the differential amplifier [F]. (D) An output of the integrator.

Fig. 11 Checking the direct-reading type interferometer by rapid density variations.

- (1) The raw fringe signal.  
(2) (A) An output of the integrator. (B) An output of the summing amplifier. (C) An output of the differential amplifier.

of this amplifier is shown in Fig. 10 (1). The RC filter, which is necessary for cutting modulation component, should not deform the envelope wave form of the fringe. Here we chose about 100 kHz as a cut-off frequency.

In order to check this circuit, we carried out the experiment, in which the fringe was produced by vibrating the one horn. Figure 10 (2) shows this results. Adjusting the gain of the polarity inverter and integrator in this circuit we obtained the following relation:

$$m = V_0 / 0.16 \quad (14)$$

where  $V_0$  is the output voltage of the integrator.

Furthermore, to check whether this system can measure the rapid density variation correctly, we carried out the following experiment by transmitting the microwave through the plasma. Figure 11 (1) shows

the detected raw fringe signal at the initial phase of discharge in the case of the steady filling pressure. Figure 11 (2) shows the output signal of the direct-reading type interferometer under the same condition. Comparing the raw fringe signal with the summing and differential signals in Fig. 11 (2), it is found that the latter signals are fed into the comparators without deformations by the RC filter. According to the Fig. 6, the relation of the integrator output signal to the summing and differential signals is considered correct. Thus, it turns out that this direct-reading type interferometer can correctly measure the rapid density variation.

#### 4. Experimental Results and Discussion

Figures 12 (1) and (2) are the example of the density variation in the case of the steady filling pressure  $P_f = 7.1 \times 10^{-4}$  Torr. The average line density reached  $5.2 \times 10^{13} \text{cm}^{-3}$  at  $200 \mu\text{s}$  and then decreased, which may be due to a low recycling ratio by the discharge cleaning. As

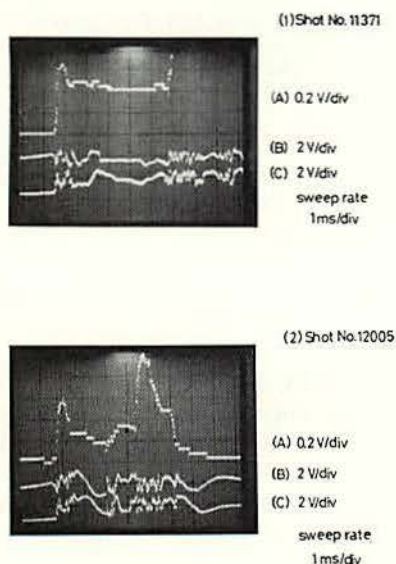


Fig. 12 Examples of the density variations in the steady filling pressure experiments ( $7.1 \times 10^{-4}$  Torr).

- (1)-(2) (A) An output of the integrator. (B) An output of the summing amplifier. (C) An output of the differential amplifier.

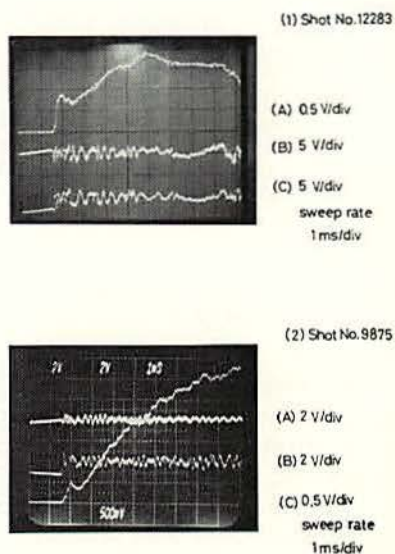


Fig. 13 Examples of the density variations in the gas puffing experiments.

- (1)-(2) (A) An output of the integrator. (B) An output of the summing amplifier. (C) An output of the differential amplifier.

shown in Fig. 12 once a current disruption occurs at about 5 ms, the density increases rapidly. This may be due to the impurity influx by the plasma wall interaction.

Figure 13 (1) shows the density variation obtained in the gas puffing experiment. We obtained the maximum average line density of about  $1.2 \times 10^{14} \text{cm}^{-3}$ , where the discharge was very stable. Figure 14 (2) also shows an example of the gas puffing experiments. Although the discharge was unstable, the maximum fringe number reached 21.8 which corresponded to  $2 \times 10^{14} \text{cm}^{-3}$ , where 4 cm plasma radius and flat distribution were assumed.

Whenever the current disruption occurred at the end of the discharge, the density increased rapidly and then decreased. In this case, however, the integrator output did not recover the zero-level. This miscounting may come from the fact that the density variation is too rapid for this direct-reading type interferometer to follow or that the output fringe signal becomes small due to the plasma displacement which leads to a microwave refraction.

We were able to measure the initial density rise in the case of the filling pressure  $P_f = 7.1 \times 10^{-4}$  Torr. However, it was difficult to measure in the case of  $P_f = 1.0 \times 10^{-3}$  Torr. This may be due to the fact that the high frequency characteristic of this direct-reading type interferometer is not enough. To use the mixer diode instead of the diode detector and construct the circuit with the higher frequency characteristic might provide a better result.

In conclusion, we constructed the high-speed direct-reading type interferometer and succeeded in measuring the rapid density variation of the TRIAM-1 tokamak plasma. The average line density of (1-20)  $10^{13} \text{cm}^{-3}$  was obtained.

#### Acknowledgments

The authors wish to thank Professor N. Yajima for his encouragement. We are also grateful to Mr. S. Kawasaki for helpful suggestions concerning electronics.

#### References

- 1) Heald, M. A. and Wharton, C. B.: *Plasma Diagnostics with Microwaves*, (John Wiley and Sons Inc., New York, London and Sydney, 1965)
- 2) Matsuura, K. and Fujita, J.: *Direct-reading Type Microwave Interferometer*, IPPJ-T-29 (1977).
- 3) Bates, D. D., Dyer, G. R. and Wing, W. R.: 140 GHz Digital Microwave Interferometer for Electron Density Measurements in ORMAK, Bull. Amer. Phys. Soc. **19** (1974) 915.
- 4) Nagashima, A., Funahashi, A. and Kawakami, T.: A 2-mm microwave Digital Interferometer for Tokamak Discharges in the Upgraded DIVA, Japanese Journal of Applied

Physics 17 (1978) 1263.

- 5) Hiraki, N., Itoh, S., Kawai, Y., Toi, K., Nakamura, K. and Mitarai, O.: *Confinement of Ohmically Heated Plasmas and Turbulent Heating in High-Magnetic-Field Tokamak TRIAM-1*, Rep. Res. Inst. Appl. Mech. 27 No. 85 (1979) 85.
- 6) Murakami, M., Callen, J. D., and Berry, L. A.: *Some Observations on Maximum Densities in Tokamak Experiments*, Nuclear Fusion, 16 (1976) 347.
- 7) Shmoys, J.: *Proposed Diagnostic Method for Cylindrical Plasmas*, Journal of Applied Physics 32 (1961) 689.

(Received December 3, 1979)